

Oxygen doping $\text{Bi}_2\text{Sr}_2\text{CaCu}_2\text{O}_{8+\delta}$ superconductors: Variations in the BiO-layer electronic states determined by scanning tunneling microscopy

Zhe Zhang and Charles M. Lieber

Harvard University, 12 Oxford Street, Cambridge, Massachusetts 02138

(Received 12 March 1992; revised manuscript received 13 May 1992)

Scanning tunneling spectroscopy (STS) and microscopy (STM) have been used to elucidate the low-energy electronic states and structure of the BiO layer in high-pressure oxygen-annealed $\text{Bi}_2\text{Sr}_2\text{CaCu}_2\text{O}_{8+\delta}$ single crystals. Our STS measurements demonstrate that oxygen doping increases the BiO layer density of states (DOS) near the Fermi level. Atomic resolution images indicate, however, that the BiO layer may not become metallic. These results provide a picture of the electronic changes in the BiO layer due to oxygen doping and elucidate the relationship between variations in the BiO layer DOS and T_c .

It is now recognized that the development of a viable description of high-temperature superconductivity in the copper oxide materials requires a detailed understanding of the normal state and how it evolves with doping.¹⁻¹² It is generally agreed that doping these materials with holes destroys the antiferromagnetic insulating state and yields a "metallic" state; however, the detailed nature of this metallic state remains controversial.^{1-4,11} One of the principle techniques that has been used to probe the normal-state electronic properties of the copper oxide superconductors is photoemission spectroscopy (PES).⁴ PES studies of $\text{Bi}_2\text{Sr}_2\text{CaCu}_2\text{O}_{8+\delta}$ have provided important data addressing the band-structure and superconducting energy gap of this system.⁴⁻¹⁰ In addition, Shen *et al.* have recently used PES to provide evidence for a chemical potential shift with oxygen doping; these results suggest that a conventional one-electron picture may be applicable to $\text{Bi}_2\text{Sr}_2\text{CaCu}_2\text{O}_{8+\delta}$.¹¹ It is important to recognize, however, that in these complex layered materials it is often difficult to distinguish which states contribute to the PES signal at the Fermi level (E_F); that is, the BiO and CuO_2 planes may contribute in $\text{Bi}_2\text{Sr}_2\text{CaCu}_2\text{O}_{8+\delta}$ and the CuO_2 planes and CuO chains can contribute in $\text{YBa}_2\text{Cu}_3\text{O}_{7-\delta}$.

To further advance our understanding of the low-energy excitations in these materials and the response of these excitations to doping it is essential to deconvolute the contributions from the distinct structural components. For $\text{Bi}_2\text{Sr}_2\text{CaCu}_2\text{O}_{8+\delta}$, scanning tunneling microscopy (STM) is uniquely suited to this task, since it can directly probe the surface BiO layer electronic states with little contribution from the underlying CuO_2 planes. Studies of this system to date have shown that the BiO surfaces of as-grown crystals are semiconducting and that Pb doping in the BiO layer does not perturb the electronic states near the Fermi level.¹³⁻¹⁶ An important problem that has not been adequately addressed for $\text{Bi}_2\text{Sr}_2\text{CaCu}_2\text{O}_{8+\delta}$ is to understand how the electronic states evolve with oxygen doping, since doping formally introduces holes into this system. Here we report STM and scanning tunneling spectroscopy (STS) studies of

$\text{Bi}_2\text{Sr}_2\text{CaCu}_2\text{O}_{8+\delta}$ single crystals that have been doped by high-pressure oxygen annealing. Recent PES studies of $\text{Bi}_2\text{Sr}_2\text{CaCu}_2\text{O}_{8+\delta}$ crystals doped in a similar way have shown that the density of states (DOS) at E_F increase with increasing δ .¹⁰ To explain this increase in the DOS it was suggested that oxygen doping transformed the BiO structural element into a metallic layer. Our STS studies also show that the DOS near E_F increases with δ ; however, atomic resolution images indicate that the BiO layer may not become metallic.

Single crystals of $\text{Bi}_2\text{Sr}_2\text{CaCu}_2\text{O}_{8+\delta}$ were grown from CuO-rich melts as described previously.¹⁶ The crystals obtained directly from the melts ("as-grown") were annealed in a high-pressure bomb at 540°C. Here we concentrate on measurements made using as-grown crystals and ones annealed in 12 atm of O_2 ("oxygen-annealed"). The values of δ were determined by thermogravimetric analysis;¹⁷ there was an increase $\Delta\delta$ of 0.33 for this oxygen-annealing procedure. X-ray diffraction measurements showed no evidence for phase decomposition in the oxygen-annealed samples. The transition temperatures of the two types of crystals were determined magnetically and found to be 83–85 K and 89 K for the as-grown and oxygen-annealed samples, respectively. These changes in T_c were observed on a number of independent crystal batches and are reproducible. The STM and STS measurements were made using home-built and commercial microscopes operated in an argon-filled glove box ($[\text{O}_2] \approx [\text{H}_2\text{O}] \approx 1$ ppm). Reproducible and stable measurements were obtained from samples cleaved *in situ*. Current (I) versus voltage (V) curves were acquired by interrupting the feedback loop and then ramping the sample-tip bias voltage while digitally storing $I(V)$. The $I-V$ data shown in the figures represent an average of four-individual curves.

Spectroscopy data obtained on cleaved as-grown and oxygen-annealed $\text{Bi}_2\text{Sr}_2\text{CaCu}_2\text{O}_{8+\delta}$ crystals are shown in Fig. 1. As discussed previously, these crystals cleave preferentially along the weakly interacting BiO/BiO double layers to yield a stable, unreconstructed BiO surface that is ideal for surface sensitive investigations.^{4,10,13-16}

Current versus tip-sample separation measurements verify that there is a well-defined tunneling barrier in these experiments [Fig. 1(b)], and thus it is possible to interpret the I - V data in a straightforward manner.¹⁸ In Figs. 1(c)–1(f) we plot the I and $(V/I)dI/dV$ versus V data obtained on the as-grown and oxygen-annealed samples, where $(V/I)dI/dV$ is proportional to the local DOS at the surface.¹⁹ A feedback stabilized junction resistance of $10^9 \Omega$ was used to set the relative tip-sample separation in these spectroscopy measurements. This junction resistance corresponds to a relatively large tip-sample separation, and thus the results should be representative of the BiO-layer DOS without a contribution from the CuO_2 state.^{15,16,20}

A key result that is immediately evident upon comparison of the data is the distinctly different I - V behavior near E_F for the as-grown and oxygen-annealed samples.

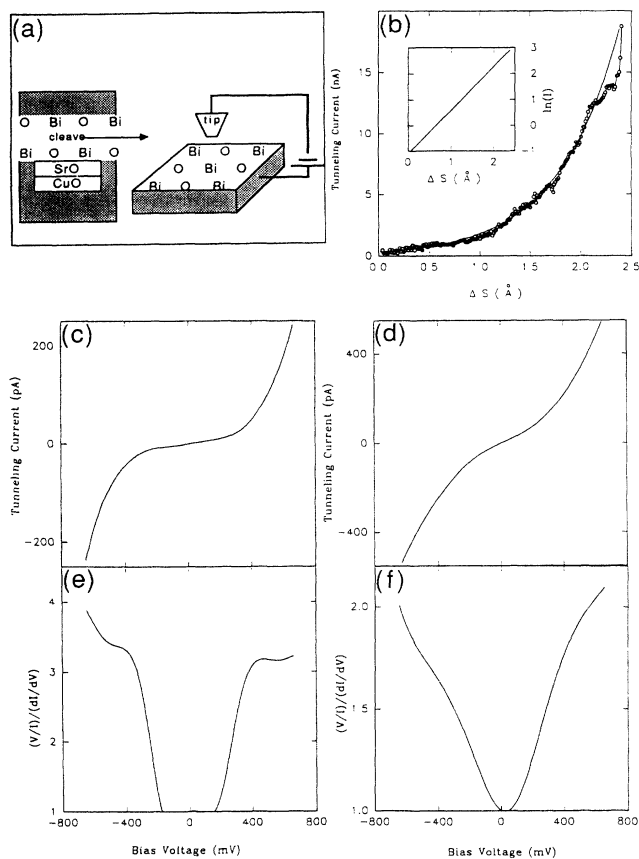


FIG. 1. (a) Schematic view of the experimental geometry for the STS studies. (b) Current vs tip-sample separation measured for a typical as-grown sample. The tip was moved directly to the surface after opening the feedback loop; the stabilized tunneling resistance was $10^9 \Omega$. The inset shows a plot of $\ln(I)$ vs distance. The apparent work function determined from these data is 2.6 eV. Typical I - V data obtained on as-grown (c) and oxygen-annealed (d) samples. The feedback stabilized tunneling resistance, $10^9 \Omega$, was the same for both experiments. Normalized conductivity curves, $(V/I)dI/dV$, corresponding to the as-grown (e) and oxygen-annealed (f) samples.

The as-grown crystals exhibit a low current within ± 200 mV of E_F and relatively sharp increases in I beyond these points, while the oxygen-annealed samples show a smooth increase in I for all V . Since the tip-sample separation is similar in both experiments, it is unlikely that this difference is due to a distance scaling effect. Indeed, the normalized conductivity $(V/I)dI/dV$ shows that there is a 330-meV gap in BiO-layer DOS for the as-grown sample, but no obvious gap for the annealed sample. The gap in the DOS observed for the as-grown crystals is similar to results reported in several independent studies and shows that this layer is semiconducting.^{14,15} The absence of a gap in the oxygen-annealed samples is significant and suggests that oxygen doping introduces states into the BiO layer near E_F . One explanation for these results is that oxygen doping introduces impurity states, which obscure an intrinsic gap in the BiO-layer DOS. Alternatively, oxygen doping may cause the BiO band to shift and cross E_F ; in this case the BiO layer will be metallic.²¹ STS measurements only provide a relative measure of the DOS, and therefore it is difficult to distinguish between these two hypotheses without additional experiments. Qualitatively, we note that the conductance dI/dV appears to be lower than that of the metallic TiO layer of $\text{Tl}_2\text{Ba}_2\text{Ca}_2\text{Cu}_3\text{O}_{10}$ crystals (see below).²²

STM imaging of the BiO-layer atomic structure provides additional information that can resolve these issues. We find that it is easier to form stable tunneling junctions at low bias voltages with the oxygen-annealed samples; this observation is consistent with the increase in BiO-layer DOS. Atomic resolution images of the as-grown and oxygen-annealed samples show, however, virtually identical surface structure (Fig. 2). The lattice for both samples has a period of $3.8 \pm 0.2 \text{ \AA}$ that corresponds to either the Bi-Bi or O-O lattice sites. The corrugations detected in these images are also similar to previous studies.^{13,15,16} In addition, similar atomic resolution images have been recorded using bias voltages between ± 500 mV. The observation of alternate lattice sites for a range of bias conditions indicates that the BiO layer is semiconducting in both as-grown and oxygen-annealed crystals. A recent STM study of the related system $\text{Tl}_2\text{Ba}_2\text{Ca}_2\text{Cu}_3\text{O}_{10}$ has shown that it is possible to image simultaneously both Tl and O sites when the surface is metallic;²² it is thus unlikely that the present results are due to an instrumental limitation. We suggest that the BiO-layer DOS near E_F increases with oxygen annealing, but that this layer remains semiconducting.²³

A previous PES study of $\text{Bi}_2\text{Sr}_2\text{CaCu}_2\text{O}_{8+\delta}$ suggested that the BiO layer becomes metallic with oxygen annealing.¹⁰ Since the PES sampling depth includes both CuO_2 and BiO layers it is possible that the Fermi-level crossing detected along Γ - M is due to a modification of the CuO_2 band and not the BiO band. It is also possible that the different conclusions obtained by STM and PES are due to intrinsic differences in the crystals, since the same oxygen annealing procedure increased the T_c of our samples to 89 K and decreased the T_c of the crystals studied by PES to 79 K. To further test this idea we have investigated $\text{Bi}_2\text{Sr}_2\text{CaCu}_2\text{O}_{8+\delta}$ crystals annealed at higher O_2 pres-

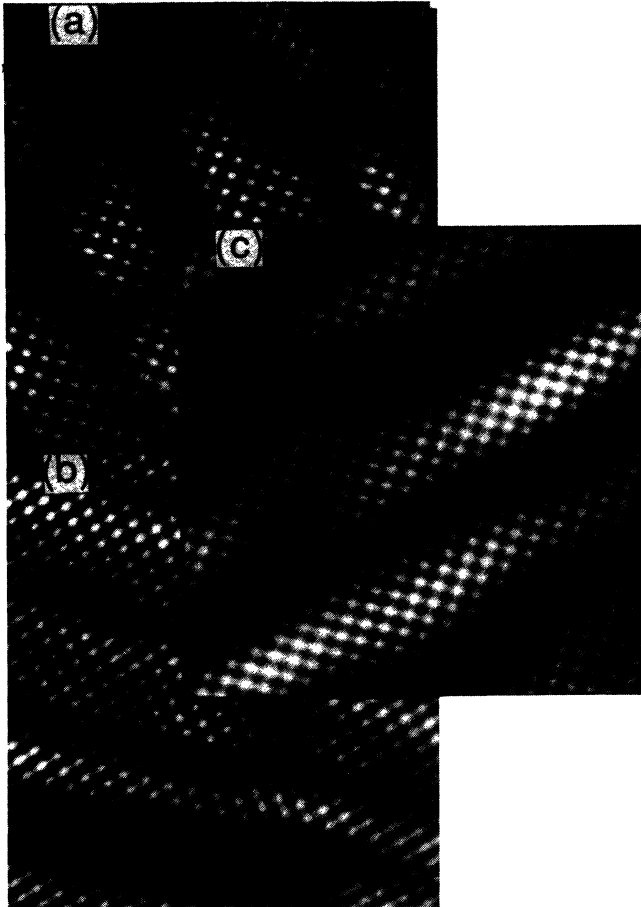


FIG. 2. $100 \times 100 \text{ \AA}^2$ STM images recorded on (a) as-grown, (b) 12-atm oxygen-annealed and (c) 150-atm oxygen-annealed $\text{Bi}_2\text{Sr}_2\text{CaCu}_2\text{O}_{8+\delta}$ cleaved single crystal. The tetragonal lattice spacing in the three images is 3.8 \AA . The images were recorded using bias voltages and tunneling currents of (a) 300 mV and 0.9 nA, (b) 250 mV and 1.8 nA, and (c) 310 mV and 1.6 nA.

tures (50–150 atm). We find that T_c decreases with increasing pressure ($P > 12$ atm); however, STM studies of these crystals indicate that the BiO layer is still semiconducting [Fig. 2(c)]. We suggest that the BiO layer remains intrinsically semiconducting with oxygen annealing, although the BiO-layer DOS at E_F does increase due

to the introduction of impurity states within the gap.

It is also important to consider the mechanism of oxygen doping in the $\text{Bi}_2\text{Sr}_2\text{CaCu}_2\text{O}_{8+\delta}$ system. From thermogravimetric analysis we know that the increase in DOS near E_F can be associated with incorporation of ≈ 0.3 oxygen/ $\text{Bi}_2\text{Sr}_2\text{CaCu}_2\text{O}_8$ unit. If this oxygen were incorporated into the BiO layer, we would expect to detect it in our images either directly as extra lattice sites or indirectly as locally distorted structure. Comparisons of the images of as-grown and oxygen-annealed samples do not exhibit evidence for such structural defects (Fig. 2). These results suggest (but do not prove) that oxygen is not incorporated directly into the BiO layer of the annealed samples. We believe that another explanation consistent with our structural and electronic data is that oxygen is incorporated into vacancy or interstitial sites in the SrO layers. This oxygen would only cause subtle changes in the BiO-layer structure and DOS, as observed in our experiments. It is also interesting that the increases in BiO-layer DOS determined by STS with increasing oxygen-annealing pressure (and δ) do not correlate well with the observed changes in T_c . These changes in T_c do correlate with the number of holes in the CuO_2 layers.²⁴ Hence, the BiO layer appears to play a limited role in determining superconductivity for this heavily doped regime.

In conclusion, STS and STM have been used to elucidate the low-energy electronic states and structure of the BiO layer in high-pressure oxygen-annealed $\text{Bi}_2\text{Sr}_2\text{CaCu}_2\text{O}_{8+\delta}$ single crystals. Our STS measurements directly demonstrate that oxygen doping increases the BiO-layer DOS near E_F . Atomic resolution images indicate, however, that the BiO layer may not become metallic. These studies also show that the changes in the BiO-layer DOS are not correlated with observed variations of T_c for this heavily doped regime. In a more general sense, our studies show how STM can be used to provide a layer-specific measure of the DOS in these complex materials and when combined with PES lead to a deeper understanding of the normal-state electronic structure and how it is perturbed with doping.

We acknowledge Z.-X. Shen (Stanford) for helpful discussions. C.M.L. acknowledges support of this work by the National Science Foundation (DMR-89-19210) and the Harvard-NSF-Materials Research Laboratory,

- ¹P. W. Anderson, in *High Temperature Superconductivity*, edited by K. S. Bedell, D. Coffey, D. E. Meltzer, D. Pines, and J. R. Schrieffer (Addison-Wesley, Redwood City, CA, 1990), p. 3.
- ²C. M. Varma, P. B. Littlewood, S. Schmitt-Rink, E. Abrahams, and A. E. Ruckenstein, *Phys. Rev. Lett.* **63**, 1996 (1989).
- ³G. A. Sawatsky, *Nature (London)* **342**, 480 (1989).
- ⁴G. Margaritondo, D. L. Huber, and C. G. Olson, *Science* **246**, 770 (1989).
- ⁵R. Manzke, T. Buslaps, R. Claessen, and J. Fink, *Europhys. Lett.* **9**, 477 (1989).
- ⁶T. Takahashi, H. Matsuyama, H. Katayama-Yoshida, Y. Okabe, S. Hosoya, K. Seki, H. Fujimoto, M. Sato, and H. Inoku-

chi, *Phys. Rev. B* **39**, 6636 (1989).

- ⁷H. Eisaki, H. Takagi, S. Uchida, H. Matsubara, S. Suga, M. Nakamura, K. Yamaguchi, A. Misu, H. Namatame, and A. Fujimori, *Phys. Rev. B* **41**, 7188 (1990).
- ⁸J.-M. Imer, F. Patthey, and B. Dardel, W.-D. Schneider, Y. Baer, Y. Petroff, and A. Zettl, *Phys. Rev. Lett.* **62**, 336 (1989).
- ⁹Y. Chang, M. Tang, R. Zanon, M. Onellion, R. Joynt, D. L. Huber, G. Margaritondo, P. A. Morris, W. A. Bonner, J.-M. Tarascon, and N. G. Stoffel, *Phys. Rev. B* **39**, 4740 (1989).
- ¹⁰B. O. Wells, Z.-H. Shen, D. S. Dessau, W. E. Spicer, C. G. Olson, D. B. Mitzi, A. Kapitulnik, R. S. List, and A. Arko, *Phys. Rev. Lett.* **65**, 3056 (1990).
- ¹¹Z.-X. Shen, D. S. Dessau, B. O. Wells, C. G. Olson, D. B.

- Mitzi, L. Lombardo, R. S. List, and A. J. Arko, *Phys. Rev. B* **44**, 12 098 (1991).
- ¹²Z. Schlesinger, R. T. Collins, F. Holtzberg, C. Feild, G. Koren, and A. Gupta, *Phys. Rev. B* **41**, 11 237 (1990).
- ¹³M. D. Kirk, J. Nogami, A. A. Baski, D. B. Mitzi, A. Kapitulnik, T. H. Geballe, and C. F. Quate, *Science* **242**, 1673 (1988).
- ¹⁴M. Tanaka, T. Takahashi, H. Katayama-Yoshida, S. Yamazaki, M. Fujinami, Y. Okabe, W. Mizutani, M. Ono, and K. Kajumura, *Nature (London)* **339**, 691 (1989).
- ¹⁵C. K. Shih, R. M. Feenstra, J. R. Kirtley, and G. V. Chandrashekar, *Phys. Rev. B* **40**, 2682 (1989); C. K. Shih, R. M. Feenstra, and G. V. Chandrashekar, *ibid.* **43**, 7913 (1991).
- ¹⁶Z. Zhang, Y. L. Wang, X. L. Wu, J.-L. Huang, and C. M. Lieber, *Phys. Rev. B* **42**, 1082 (1990); X. L. Wu, Z. Zhang, Y. L. Wang, and C. M. Lieber, *Science* **248**, 1211 (1990).
- ¹⁷D. B. Mitzi, L. W. Lombardo, A. Kapitulnik, S. S. Laderman, R. D. Jacowitz, *Phys. Rev. B* **41**, 6564 (1990).
- ¹⁸N. D. Land, *Phys. Rev. B* **34**, 5947 (1986).
- ¹⁹R. M. Feenstra, J. A. Stroscio, and A. P. Fein, *Surf. Sci.* **181**, 295 (1987).
- ²⁰For small tip-sample separations it has been suggested that the CuO₂-layer DOS are also detected by tunneling (see Refs. 15 and 16). Previously, we have observed an anomalous increase in the DOS at E_F for tunneling resistances $< 10^8 \Omega$; at larger resistances no anomalous increases are observed. In this case, which corresponds to the present study, we believe that only the BiO-layer makes a significant contribution to the STS data.
- ²¹Preliminary temperature-dependent STS measurements indicate, however, that a gap opens in the BiO-layer DOS of the oxygen annealed crystals as the sample are cooled below room temperature.
- ²²Z. Zhang, C.-C. Chen, C. M. Lieber, and B. Morosin, D. S. Ginley, and E. L. Venturini, *Phys. Rev. B* **45**, 987 (1992).
- ²³Because the partial DOS could be peaked on either atomic site in a metallic system, the STM images do not completely rule out the idea that the BiO-layer becomes metallic with oxygen doping.
- ²⁴Y. L. Wang and C. M. Lieber (unpublished results).

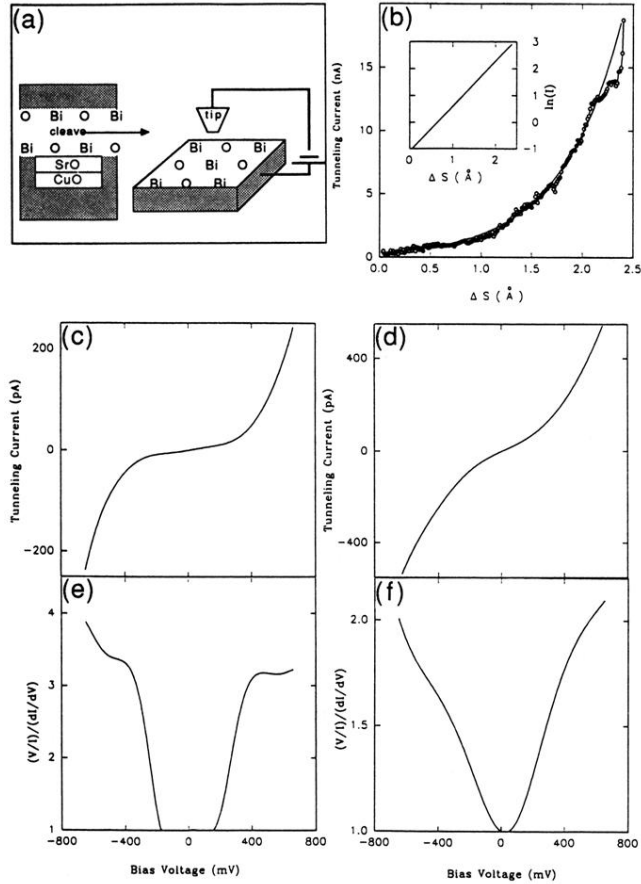


FIG. 1. (a) Schematic view of the experimental geometry for the STS studies. (b) Current vs tip-sample separation measured for a typical as-grown sample. The tip was moved directly to the surface after opening the feedback loop; the stabilized tunneling resistance was $10^9 \Omega$. The inset shows a plot of $\ln(I)$ vs distance. The apparent work function determined from these data is 2.6 eV. Typical I - V data obtained on as-grown (c) and oxygen-annealed (d) samples. The feedback stabilized tunneling resistance, $10^9 \Omega$, was the same for both experiments. Normalized conductivity curves, $(V/I)dI/dV$, corresponding to the as-grown (e) and oxygen-annealed (f) samples.

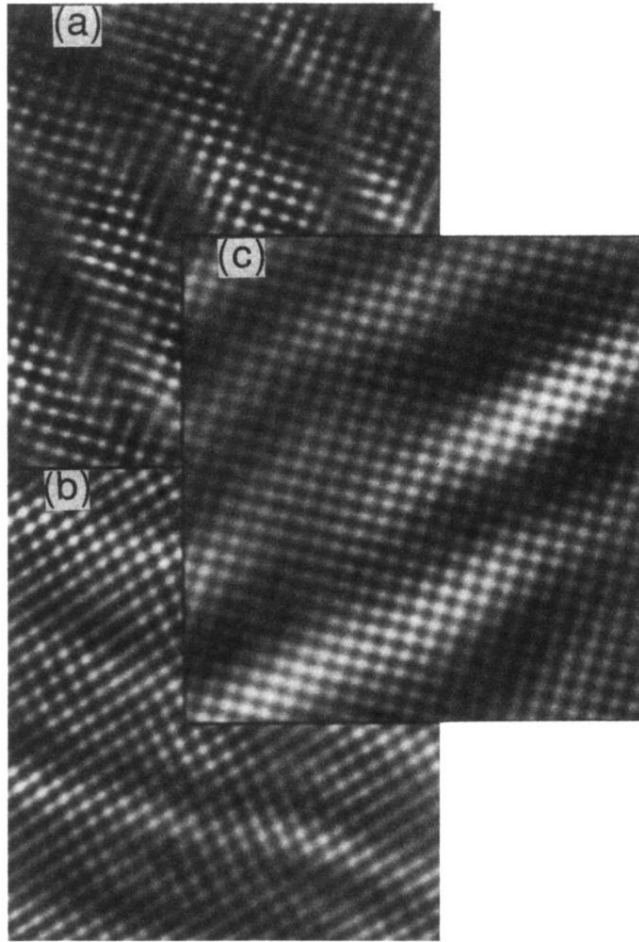


FIG. 2. $100 \times 100 \text{ \AA}^2$ STM images recorded on (a) as-grown, (b) 12-atm oxygen-annealed and (c) 150-atm oxygen-annealed $\text{Bi}_2\text{Sr}_2\text{CaCu}_2\text{O}_{8+\delta}$ cleaved single crystal. The tetragonal lattice spacing in the three images is 3.8 \AA . The images were recorded using bias voltages and tunneling currents of (a) 300 mV and 0.9 nA, (b) 250 mV and 1.8 nA, and (c) 310 mV and 1.6 nA.